Cancer Imaging (2013) **13(1),** 100–112
DOI: 10.1102/1470-7330.2013.0010

CI

e-med
www.e-med.org.uk

CASE SERIES

Ophthalmologic abnormalities on FDG-PET/CT: a pictorial essay

Razi Muzaffar[a], Mohamed A. Shousha[b], Lejla Sarajlic[c], Medhat M. Osman[a,d]

[a]Department of Radiology, Division of Nuclear Medicine, St Louis University, 3635 Vista Avenue, Saint Louis, MO 63110, USA; [b]Department of Ophthalmology, St Louis University, St Louis University, 3635 Vista Avenue, Saint Louis, MO 63110, USA; [c]Doisy College of Health Sciences, St Louis University, 3437 Caroline Street, Saint Louis, MO 63104, USA; [d]Department of Radiology, Division of Nuclear Medicine, John Cochran VA Medical Center, St. Louis, MO, USA

Corresponding address: Medhat M. Osman, MD, MS, PhD, Saint Louis University, Department of Radiology/Division of Nuclear Medicine, Saint Louis VA Medical Center, 3635 Vista Avenue, 2-DT, St. Louis, MO 63110, USA.
Email: mosman@slu.edu

Date accepted for publication 19 December 2012

Abstract

Positron emission tomography (PET) using [^{18}F]-2-deoxy-D-glucose (FDG) diagnoses, stages, and restages many cancers and is often better than anatomic imaging alone. However, abnormalities within the orbit present a challenge in evaluation, mainly due to the subtle findings on PET/computed tomography (CT). In addition, this region is typically at the edge of the field of view for the standard base of skull to upper thigh FDG-PET/CT scans. The aim of this pictorial essay is to illustrate several subtle and apparent abnormalities within the orbit that can have a profound impact on patient management and follow-up.

Keywords: *PET/CT; ocular; eye; [^{18}F]-2-deoxy-D-glucose; FDG.*

Introduction

Positron emission tomography (PET) using [^{18}F]-2-deoxy-D-glucose (FDG) diagnoses, stages, and restages many cancers and is often better than anatomic imaging alone. The fusion of functional (PET) and anatomic computed tomography (CT) imaging continues to evolve and provide valuable clinical information. These findings, however, may be subtle on either modality alone. This is especially apparent when dealing with abnormalities within the orbit. Not only is it at the edge of the field of view for the standard base of skull to upper thigh scans, but there is also increased FDG uptake in the extraocular muscles[1]. In this article, we demonstrate various orbital abnormalities. A total of 8430 PET/CT reports were reviewed from August 2006 to June 2011. A log recorded cases of abnormalities reported within the orbit. A total of 35 patients had abnormalities described in the reports. All images were reviewed and the most interesting with all available follow-up data were selected. To the best of our knowledge, this pictorial essay may be the first to compile various abnormalities within the orbit.

PET/CT image acquisition

An intravenous injection of 5.18 MBq/kg (0.14 mCi/kg) of FDG was performed after at least a 4-h fast. Patients sat in a quiet injection room without talking during the subsequent 60 min of the FDG uptake phase and allowed to breathe normally during image acquisition. All scans were acquired using a PET/CT scanner (Gemini; Philips Medical Systems).

The CT scan component of the PET/CT scanner consisted of a 64-slice multidetector helical CT with a gantry port of 70 cm. Parameters were as follows for 20–21 bed acquisitions: 120–140 kV and 33–100 mAs (based on body mass index), 0.5 s per CT rotation, pitch of 0.9 and 512×512 matrix. CT data were used for image fusion and the generation of the CT transmission map. Arms were placed above the head for CT acquisition, except in head and neck cases where the arms were placed at the sides. Per our protocol, the CT images were obtained without oral or intravenous contrast.

The PET component of the PET/CT scanner is composed of lutetium-yttrium oxyorthosilicate (LYSO)-based crystals. Emission data were acquired on average for

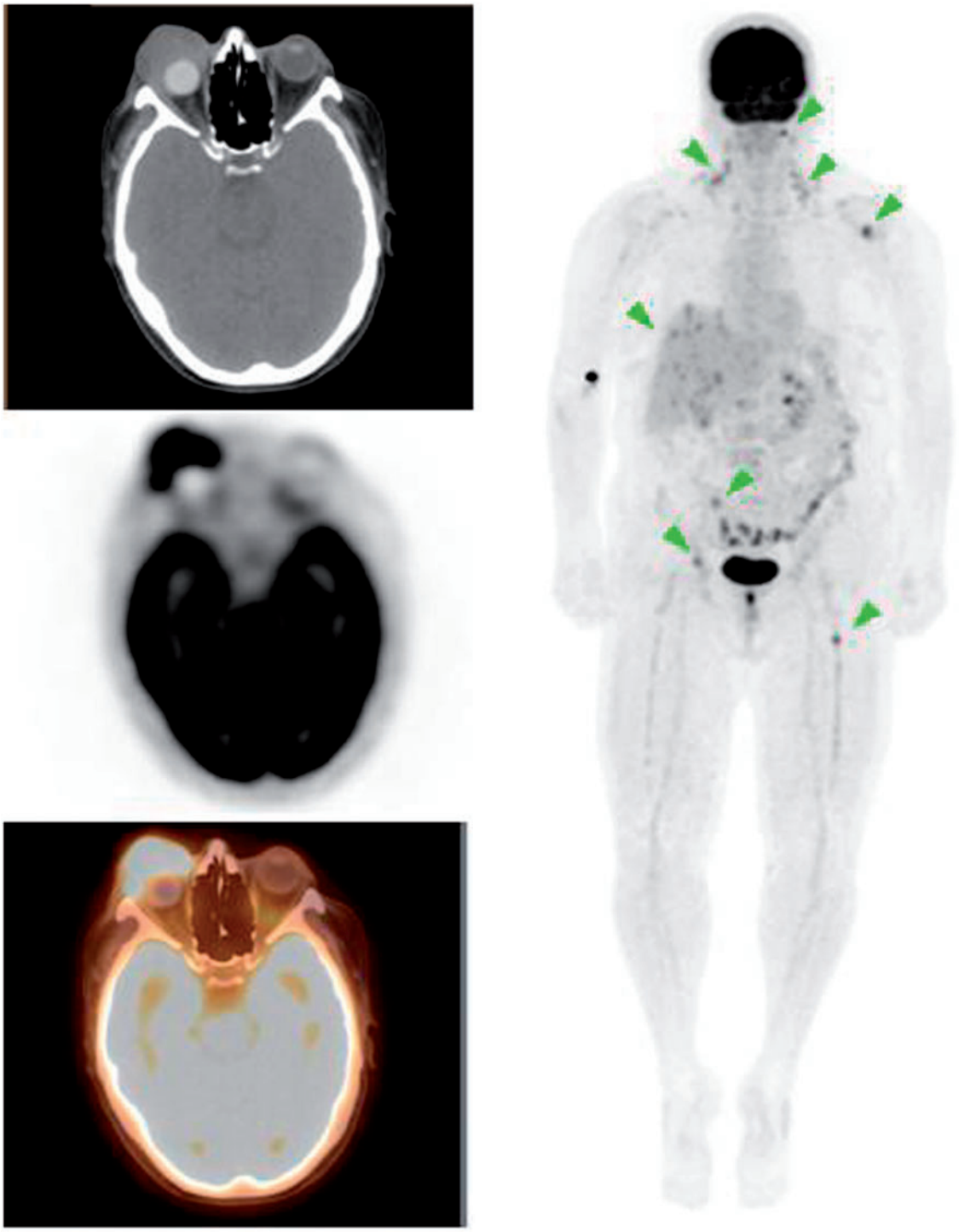

Figure 1 **A 59-year-old woman with a history of melanoma of the right eye status post enucleation with orbital implant. PET/CT images demonstrated widespread metastasis involving the cervical nodes, liver and bones. There was also a hyperdensity in the orbital cavity consistent with orbital implant and an intense FDG-avid soft tissue mass anterior to the implant (maximum standardized uptake value [SUV_{max}] 9.6). The mass was biopsied revealing malignant melanoma.**

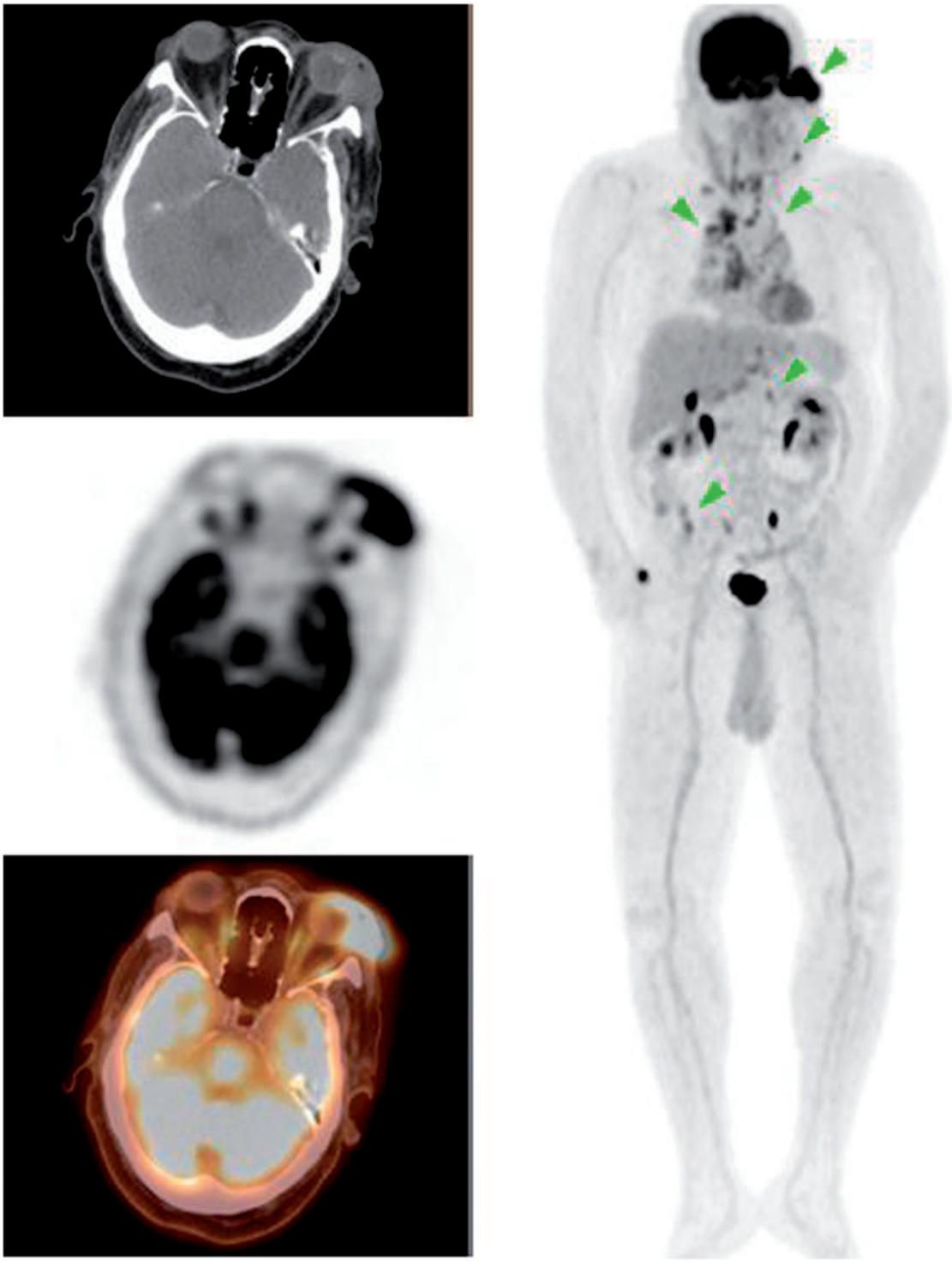

Figure 2 **A 65-year-old man presenting with a left orbital mass. PET/CT demonstrates an FDG-avid left orbital mass (SUV_{max} 11.0) with additional cervical, mediastinal and abdominal lymphadenopathy. Biopsy of the left orbital mass demonstrated squamous cell carcinoma.**

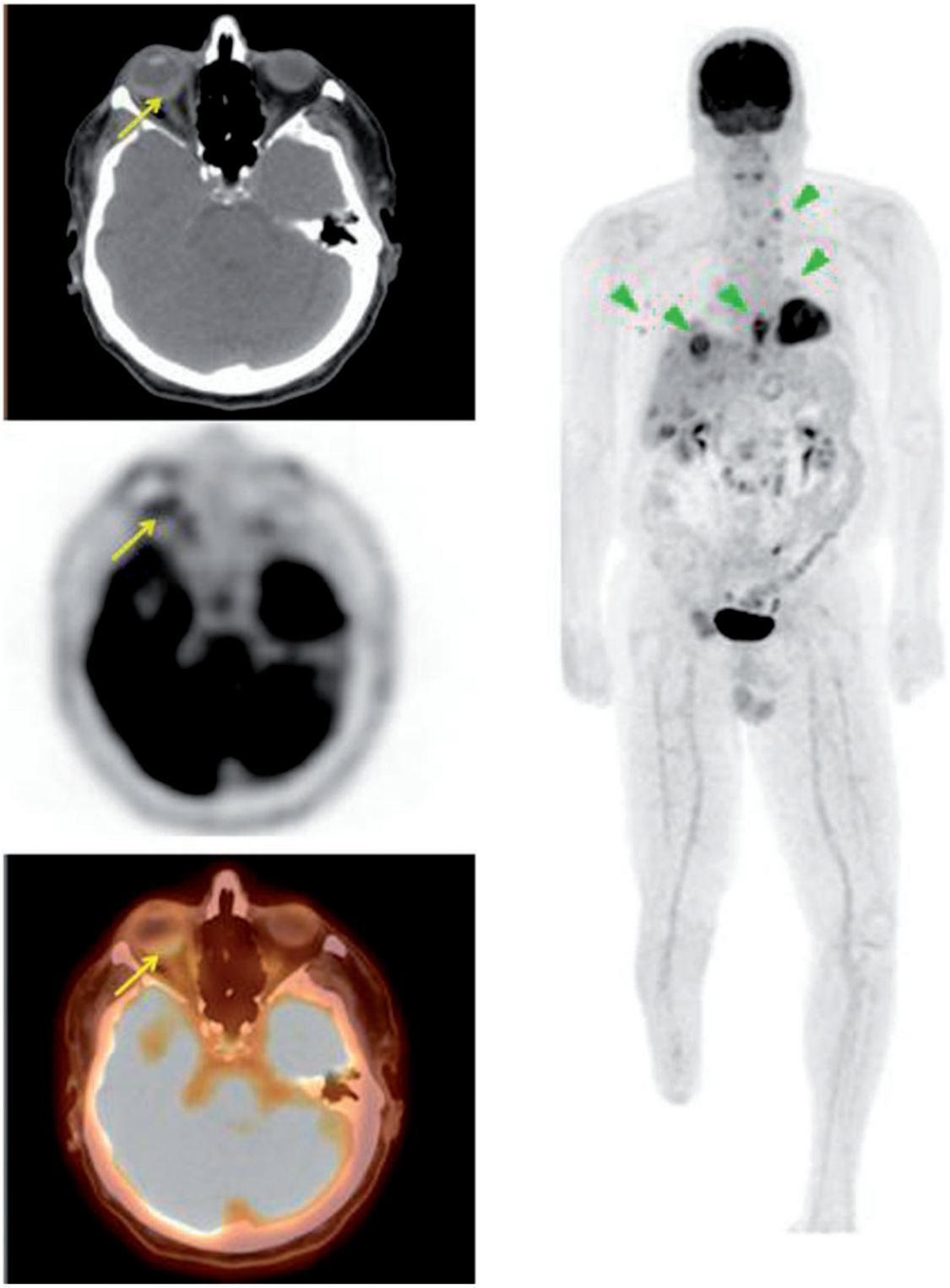

Figure 3 **A 19-year-old man with a history of esophageal cancer. PET/CT demonstrates widespread metastasis including prominent focal FDG uptake in the posterior right eye (SUV_{max} 4.0). Fine-needle aspiration of the right eye demonstrated adenocarcinoma consistent with metastasis from the esophagus.**

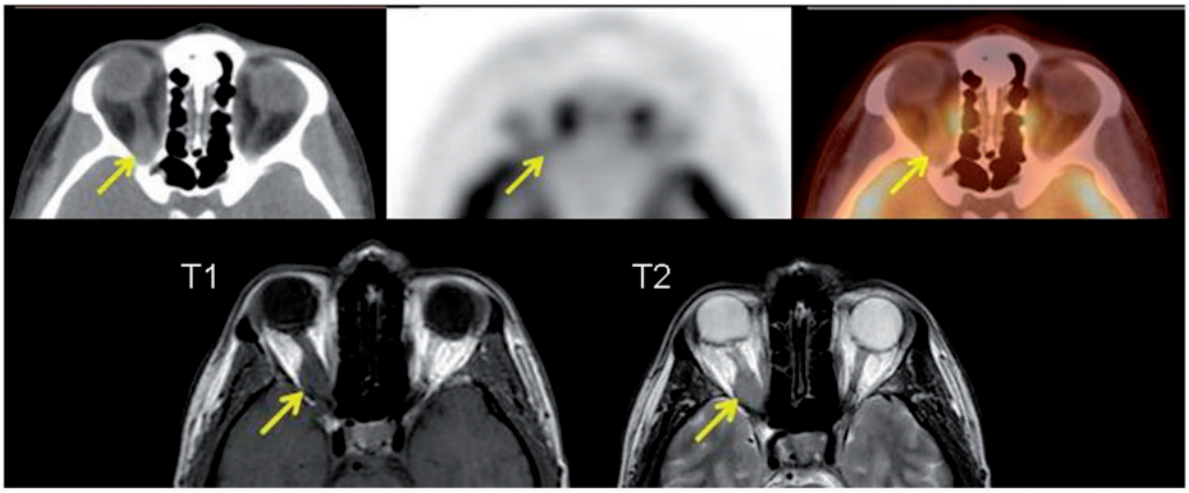

Figure 4 **A 76-year-old man with a history of lymphoma initially diagnosed from a right parotid mass. PET/CT demonstrated a soft tissue density in the superolateral right orbit (SUV_{max} 2.7) with no other lesion. Biopsy of the right orbit lesion revealed small lymphocytic lymphoma, a type of B-cell lymphoma.**

20–21 bed positions (193 cm coverage, identical to the CT protocol). Emission scans were acquired at 1–2 min per bed position. The filed of view was from the top of the head to the bottom of the feet in all patients. The three-dimensional (3D) whole-body acquisition parameters consisted of a 128×128 matrix and an 18-cm field of view with a 50% overlap. Processing consisted of the 3D Row Action Maximum Likelihood Algorithm (RAMLA) method. Total scan time per patient was 20–45 min.

Ocular tumors

Ocular cancers can be an isolated tumor originating within the globe or metastasis from another site. Tumors can be both sight and life threatening. The most common primary tumors of the eye are uveal melanoma and primary intraocular lymphoma in adults and retinoblastoma in children[2,3]. Uveal melanomas are classified according to the part of the uvea where the tumor arises, choroidal, ciliary body and iris (Fig. 1). Treatment of uveal melanoma is based on many factors, but the most important is the size of the tumor. Commonly these lesions are treated with plaque brachytherapy, but enucleation is required in severe cases.

Ocular squamous cell carcinoma is another primary ocular tumor; it is less common and arises from abnormal epithelial cells that invade the conjunctival stroma. These lesions can invade the anterior chamber of the eye or the orbital septum to involve the soft tissue of the orbit (Fig. 2). The management of this tumor is dependent on the extent of the lesion but most commonly includes excision with cryotherapy and/or chemotherapy[4,5]. These tumors typically demonstrate intense FDG uptake on PET.

Malignancies from other parts of the body also metastasize to the globe. These are usually discovered when the tumor affects vision or displaces the globe. The most common location for ocular metastasis is within the choroid, the most vascular layer of the eye (Fig. 3). This type of metastasis occurs most commonly from lung cancer in males and breast cancer in females[6]. Treatment is based on the type and severity of tumor involvement. These tumors can demonstrate variable uptake on PET depending on FDG avidity of the primary malignancy.

Orbital tumors

The orbit is a cone-shaped space comprised of seven bones (frontal, greater and lesser wings of the sphenoid, zygoma, maxilla, lacrimal, palatine, and ethmoid). It contains the globe, muscles, fat, vasculature, nerves, glands and connective tissues. Due to the confined space, a lesion can lead to proptosis affecting vision and extraocular muscle function.

Lymphoma is the most common orbital malignancy accounting for 55% of all malignant orbital tumors in adults[7]. It is a type of non-Hodgkin lymphoma that typically occurs in older patients, mostly the B-cell phenotype (Fig. 4). It presents with decreased vision and nonresolving uveitis and is usually treated with radiotherapy and/or chemotherapy[8]. These tumors typically demonstrate intense FDG uptake on PET.

Optic nerve sheath meningiomas are benign tumors of the optic nerve. They arise from the meningothelial cap cells of the arachnoid villi. As the tumor grows, it compresses the optic nerve, which causes loss of vision (Fig. 5). In older patients, management of these tumors is conservative. Radiation is the most common form of treatment. However, in younger patients, the lesions can be more aggressive and are excised. Nevertheless, optic

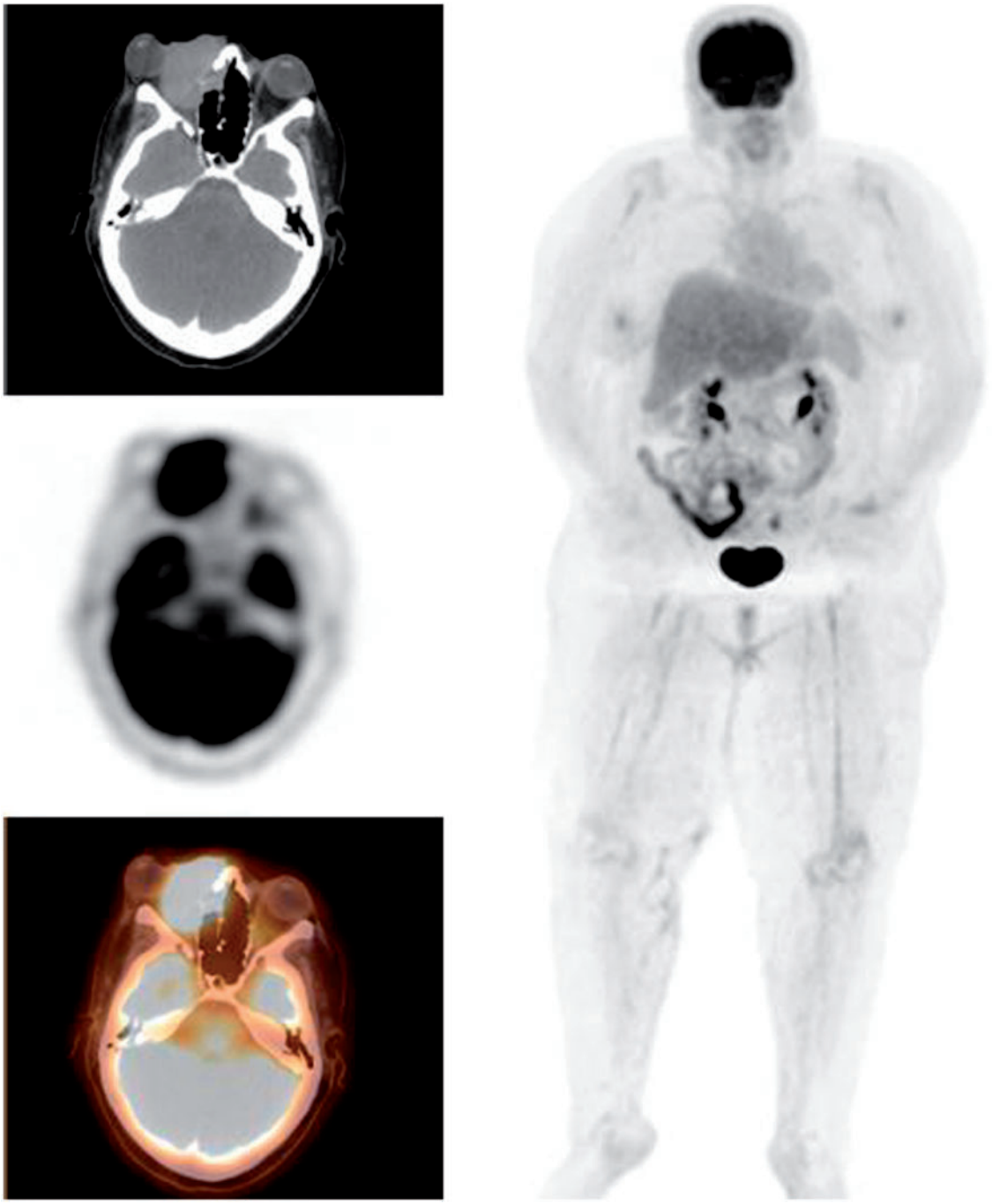

Figure 5 **A 43-year-old woman presenting with loss of vision due to a right orbital tumor. PET/CT (top row) demonstrated asymmetric thickening with mild FDG uptake in the right optic nerve. MRI was performed (bottom row). T1 and T2 images demonstrate a right intraorbital mass encasing the optic nerve isointense on T1 and T2. The mass was then biopsied revealing meningioma.**

nerve sheath meningiomas often cause severe visual deficits after resection[9]. These tumors demonstrate minimal to no FDG uptake on PET and require diagnosis from physical examination and anatomic imaging, such as magnetic resonance imaging (MRI) as in our case.

Adenoid cystic carcinoma is a tumor affecting various glands. When it involves the lacrimal gland, there is a progressive onset of proptosis, globe displacement and commonly lytic bone involvement. Pain and numbness are also common due to invasion of the local nerves (Fig. 6). The management of this tumor is typically aggressive resection with removal of soft tissue and bone followed by radiotherapy[10]. These tumors typically demonstrate intense FDG uptake on PET.

The presence of orbital metastasis is usually associated with a poor prognosis due to likely widespread

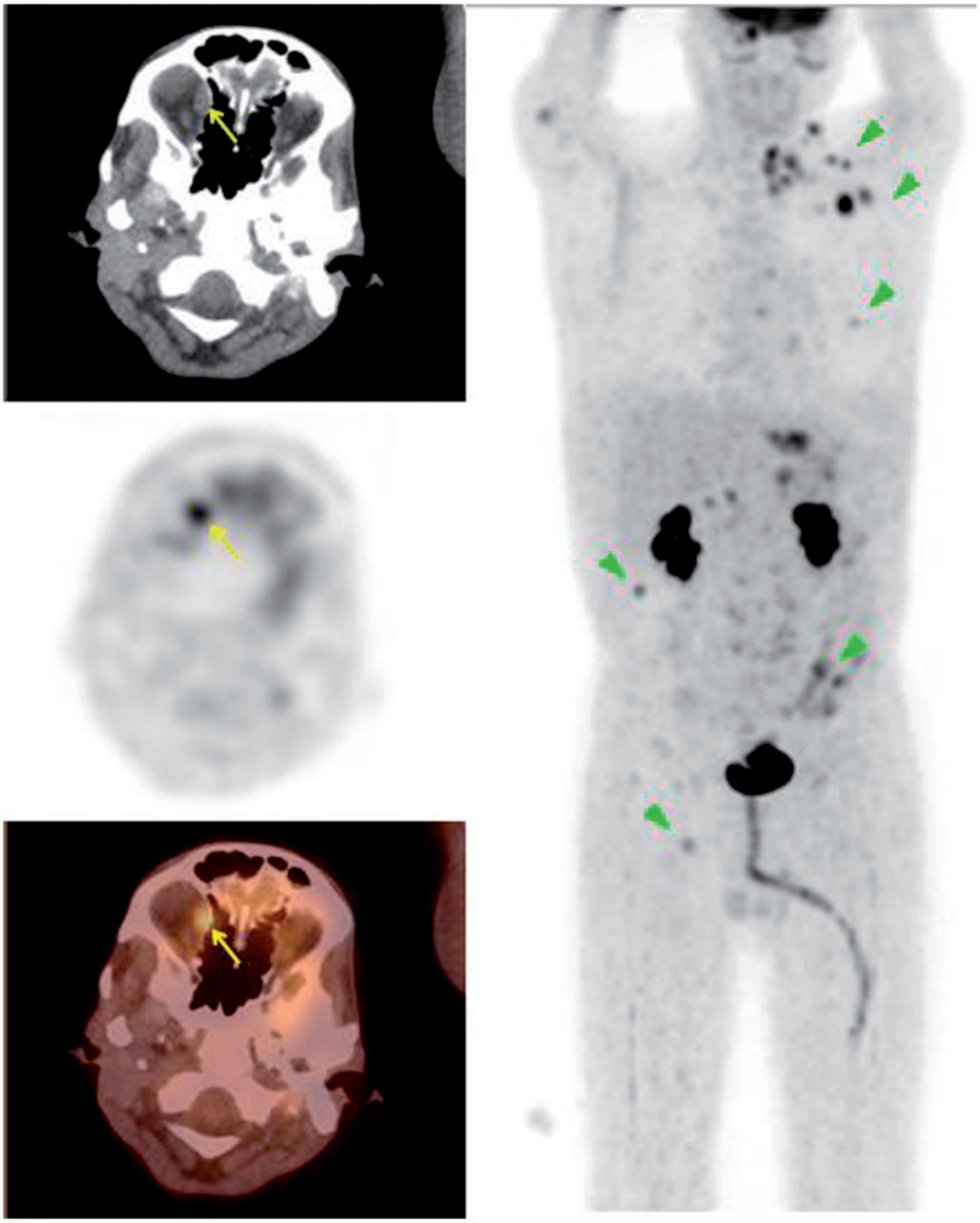

Figure 6 **A 48-year-old woman presenting with a right orbital mass. PET/CT demonstrates an FDG-avid mass within the medial right orbit (SUV_{max} 9.9) with associated bone invasion. The mass was biopsied revealing adenocarcinoma arising from the lacrimal gland, consistent with adenoid cystic carcinoma.**

malignancy (Fig. 7). The incidence of orbital metastasis is increasing, which may be due to the increased survival rate of cancer patients from improved treatment. The most common primary malignancy associated with orbital metastasis is from breast cancer (28.5–58.8%) followed by lung cancer (8–12%)[11]. Metastasis from breast cancer can cause movement deficits due to involvement of the extraocular muscles and surrounding fat. Metastasis from lung cancer is more aggressive with displacement of the globe. Orbital metastasis of cutaneous malignant melanoma occurs in 5.3–15% of all metastatic orbital tumors[11]. It often involves the extraocular muscles resulting in diplopia (Figs. 1 and 8). Surgical resection may be warranted for palliative measures and various trials of immunotherapy and chemotherapy are available[12]. These tumors can demonstrate variable

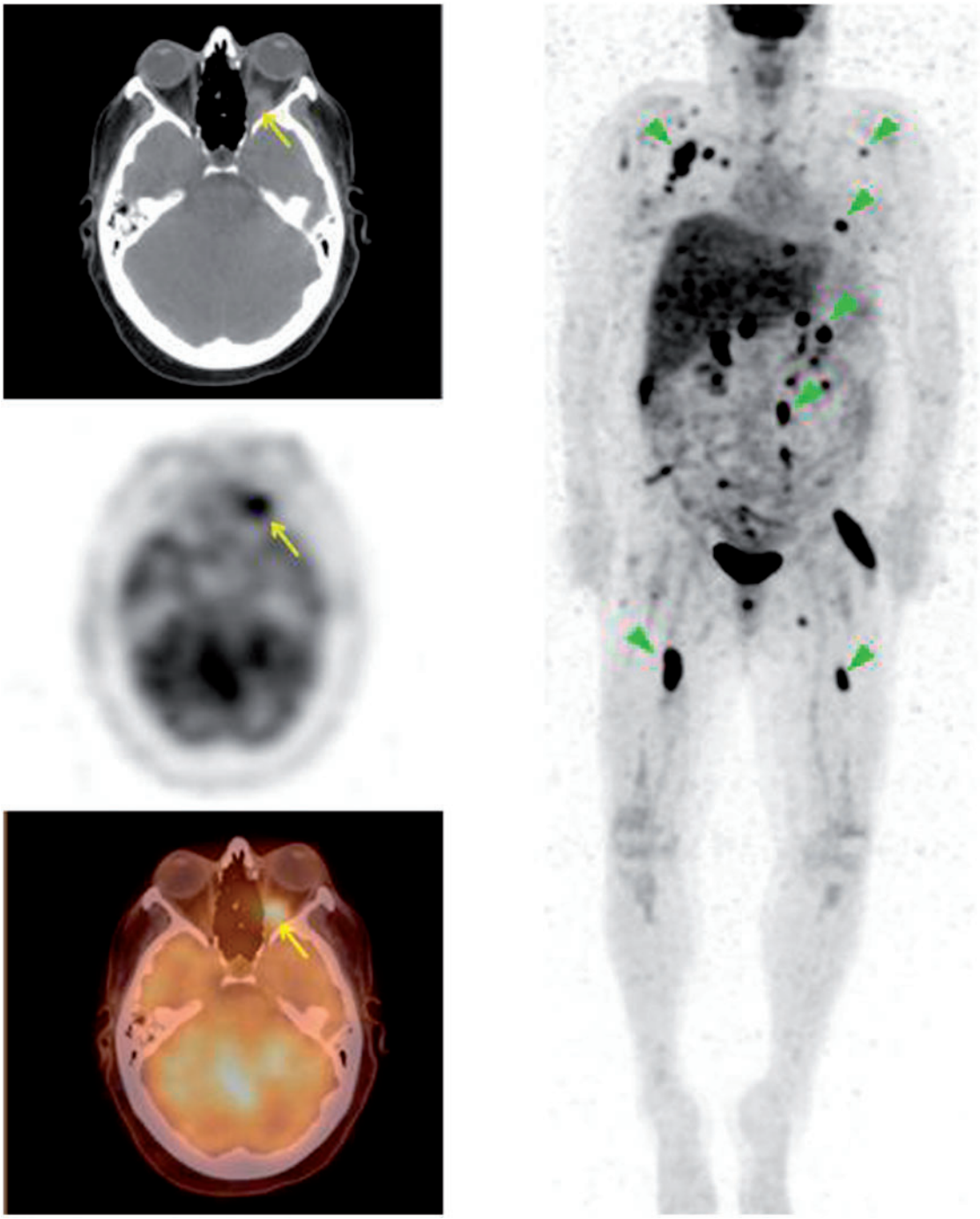

Figure 7 **A 52-year-old man presenting with abdominal adenopathy and blastic bone lesions on CT with unknown primary. PET/CT demonstrated widespread malignancy including an FDG-avid lesion in the right medial orbit with associated soft tissue thickening as seen above (SUV_{max} 4.8). Biopsy of a chest wall node revealed poorly differentiated non-small cell carcinoma with neuroendocrine features suggestive of a gastrointestinal primary.**

uptake on PET depending on FDG avidity of the primary malignancy.

Ocular implants and prosthesis

An ocular prosthesis is an artificial implant placed in an empty eye socket following an enucleation, evisceration or orbital exenteration. Implants and prosthetics are commonly used in the management of patients with intraocular tumors, trauma and disfigured eyes (Fig. 9). Hydroxyapatite implants are the most common type due to their porous nature allowing for ingrowth of host fibrovascular tissue reducing the risk of migration, extrusion and infection[13]. The implant supports the prosthesis, which is a convex shell that fits over it

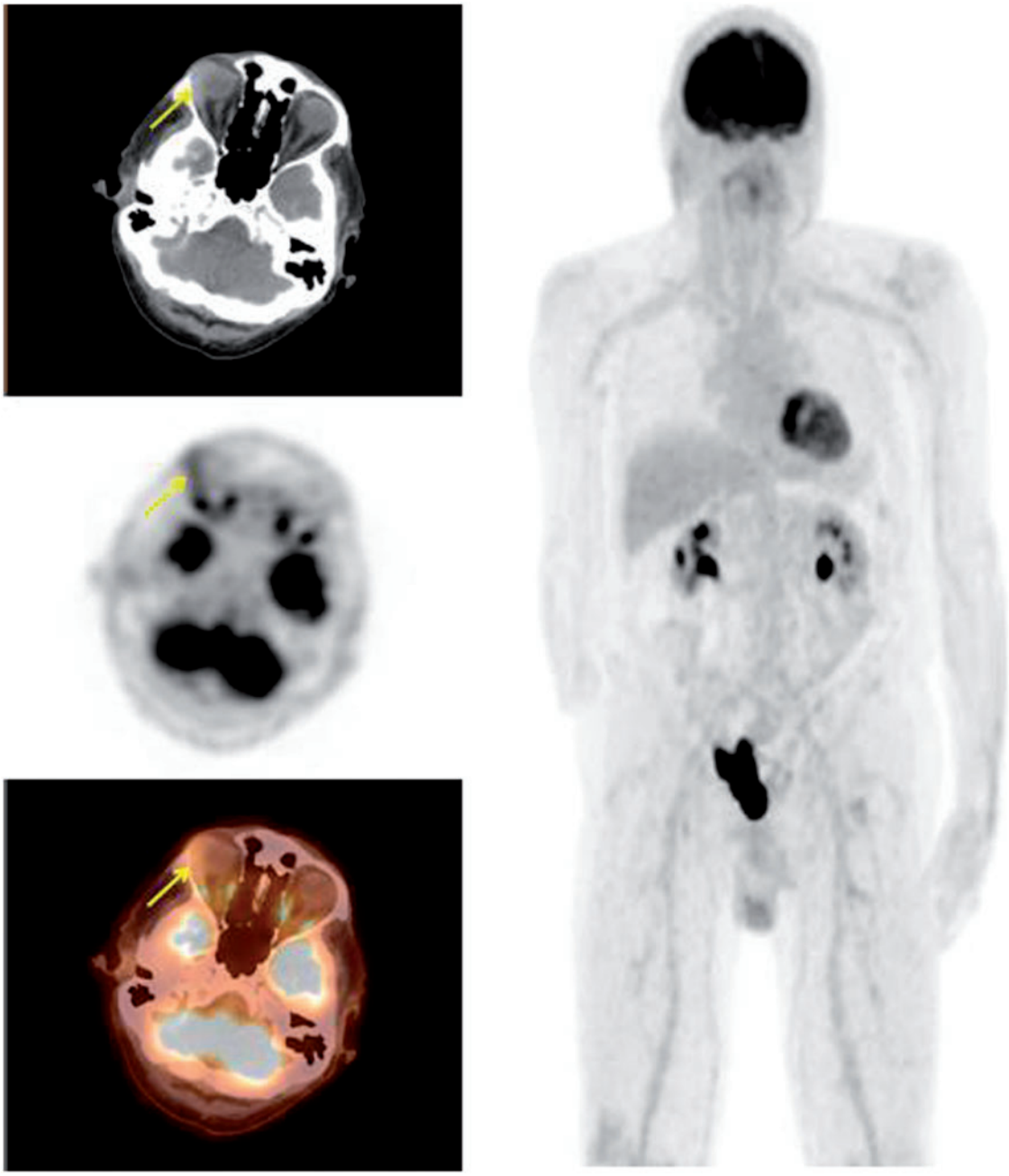

Figure 8 **A 40-year-old woman with a history of melanoma. PET/CT demonstrated widespread metastasis involving the cervical, supraclavicular, mediastinal, axillary, abdominal spaces and bone. There was also a soft tissue lesion in the posterior left orbital cavity (SUV_{max} 5.0).**

(Figs. 9 and 10). The prostheses typically demonstrate no FDG uptake on PET.

Retinal detachment is a disorder of the eye in which there is separation of the light sensitive retina in the back of the eye from the supporting layers leading to retinal tissue death and permanent vision loss. The most common form of treatment for retinal detachment is vitrectomy. It involves removing the vitreous humor from the eye and refilling it with silicon oil to reattach the retina[14,15]. However, there is an increased risk of glaucoma in these patients but this can be treated with a glaucoma shunt (Fig. 11).

Conclusion

FDG-PET/CT is a valuable tool in diagnosing and staging various types of cancers. Whether the findings are apparent or very subtle, as in the case of abnormalities within the orbit, they can have a profound impact on patient management and appropriate follow-up.

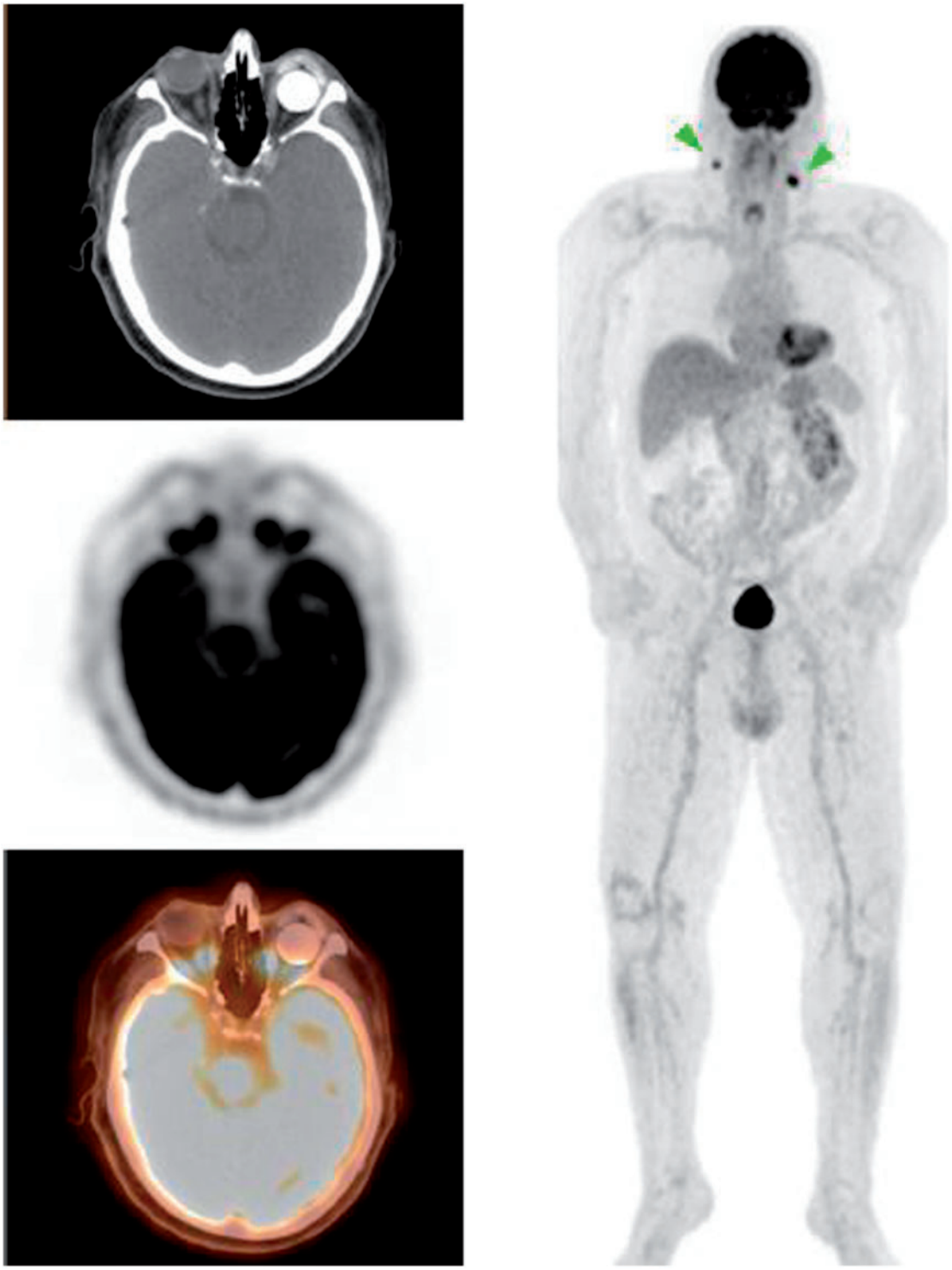

Figure 9 **A 72-year-old man with a history of recurrent squamous cell carcinoma of the left nasal cavity requiring enucleation. A left ocular implant and prosthesis was seen at the time of scanning as well as FDG-avid bilateral cervical lymph nodes. An ocular implant was placed immediately after the enucleation represented by the non-FDG-avid circular hyperdensity in the orbit. The prosthesis sits anterior to the implant.**

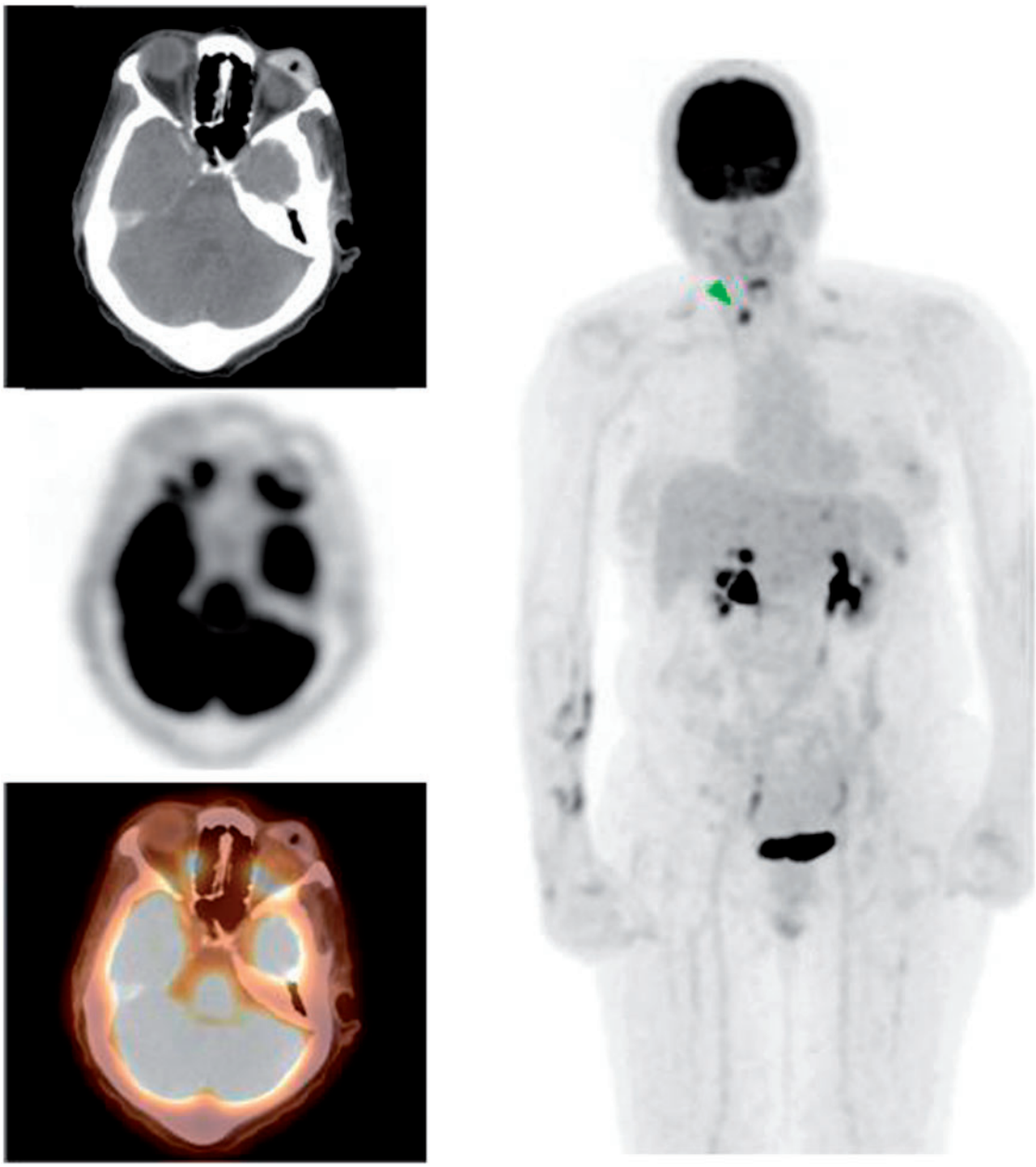

Figure 10 **A 64-year-old woman with a history of squamous cell carcinoma of the oropharynx. Images demonstrated normal variant FDG uptake in the larynx, focal FDG uptake in the right lobe of the thyroid gland and left phthisis bulbi (shrunken, non-functional eye) with a non-FDG-avid prosthesis anterior to it. At times, a plastic scleral shell may be used to treat phthisis bulbi or microphthalmia.**

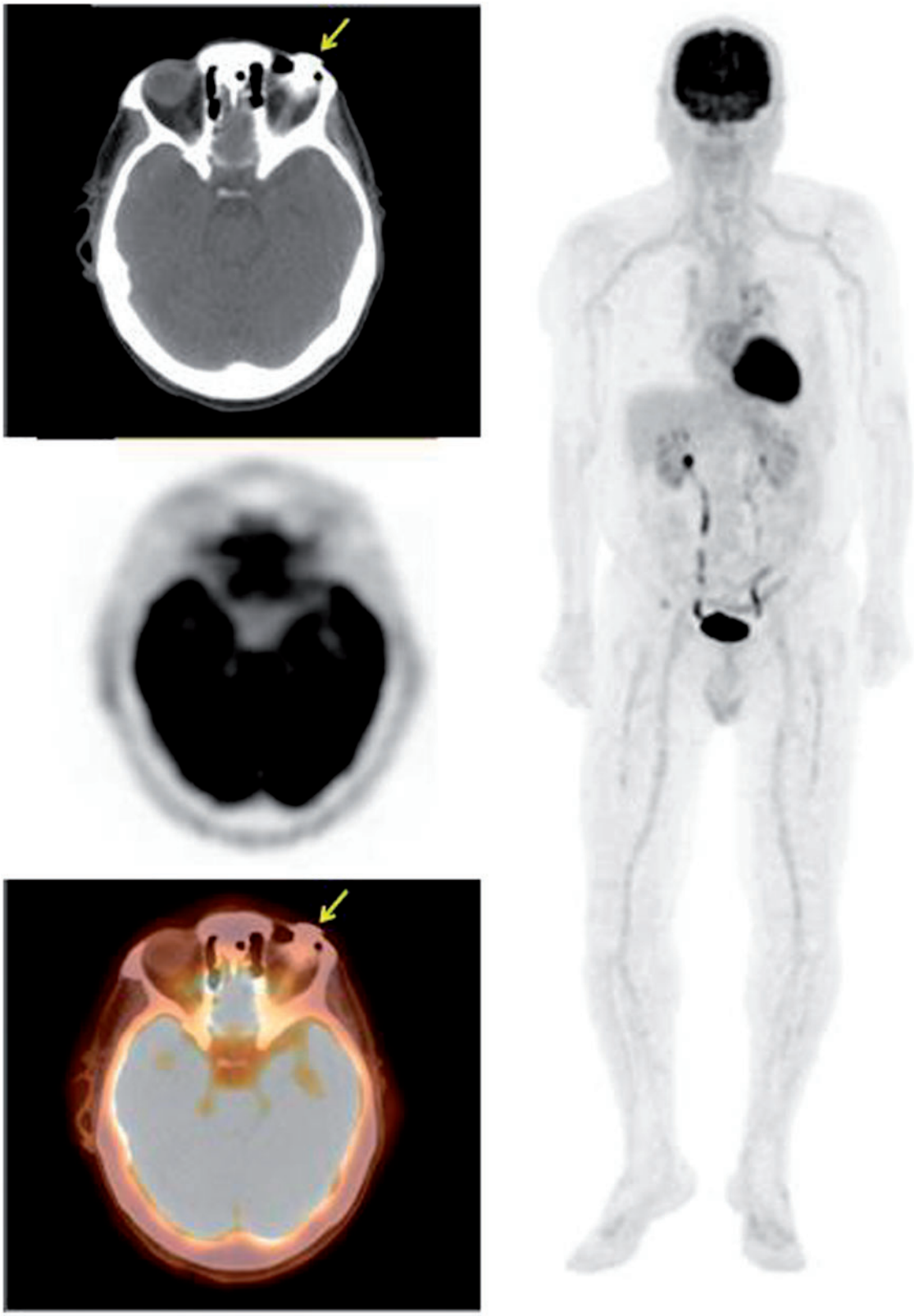

Figure 11 **A 77-year-old man presenting with non-small cell lung cancer with a history of retinal detachment. PET/CT images demonstrate a non-FDG-avid hyperdense foreign material in the superior aspect of the left eye. The most common form of treatment for retinal detachment is vitrectomy, such as in this case. It involves removing the vitreous fluid from the eye and refilling it with silicon oil to reattach the retina. The left globe is also more dense than the right (22 HU vs 11 HU) due to the differences in fluid. However, there is an increased risk of glaucoma in these patients but it can be treated with a glaucoma shunt, seen as the hyperdensity in this case.**

References

[1] Shreve PD, Anzai Y, Wahl RL. Pitfalls in oncologic diagnosis with FDG PET imaging: physiologic and benign variants. Radiographics 1999; 19: 61–77; quiz 150–151. PMid:9925392.

[2] Singh P, Singh A. Choroidal melanoma. Oman J Ophthalmol 2012; 5: 3–9. doi:10.4103/0974-620X.94718. PMid:22557869.

[3] Rosado MF, Byrne GE, Jr. Ding F, et al. Ocular adnexal lymphoma: a clinicopathologic study of a large cohort of patients with no evidence for an association with *Chlamydia psittaci*. Blood 2006; 107: 467–472. doi:10.1182/blood-2005-06-2332. PMid:16166588.

[4] Finger PT, Chin KJ. Refractory squamous cell carcinoma of the conjunctiva treated with subconjunctival ranibizumab (Lucentis): a two-year study. Ophthal Plast Reconstr Surg 2012; 28: 85–89. doi:10.1097/IOP.0b013e3182392f29. PMid:22186988.

[5] Yousuf YA, Finger PT. Squamous carcinoma and dysplasia of the conjunctiva and cornea. Ophthalmology 2012; 119: 233–240. doi:10.1016/j.ophtha.2011.08.005.

[6] Shields CL, Shields JA. Tumors of the conjunctiva and cornea. Surv Ophthalmol 2004; 49: 3–24. doi:10.1016/j.survophthal.2003.10.008. PMid:14711437.

[7] Valvassori GE, Sabnis SS, Mafee RF, Brown MS, Putterman A. Imaging of orbital lymphoproliferative disorders. Radiol Clin North Am 1999; 37: 135–150, x–xi. doi:10.1016/S0033-8389(05)70083-X. PMid:10026734.

[8] Demirci H, Shields CL, Shields JA, Honavar SG, Mercado GJ, Tovilla JC. Orbital tumors in the older adult population. Ophthalmology 2002; 109: 243–248. doi:10.1016/S0161-6420(01)00932-0. PMid:11825802.

[9] Saeed P, Rootman J, Nugent RA, White VA, Mackenzie IR, et al. Optic nerve sheath meningiomas. Ophthalmology 2003; 110: 2019–2030. doi:10.1016/S0161-6420(03)00787-5. PMid:14522782.

[10] Fordice J, Kershaw C, El-Naggar A, et al. Adenoid cystic carcinoma of the head and neck: predictors of morbidity and mortality. Arch Otolaryngol Head Neck Surg 1999; 125: 149–152. PMid:10037280.

[11] Ahmad SM, Esmaeli B. Metastatic tumors of the orbit and ocular adnexa. Curr Opin Ophthalmology 2007; 18: 405–413. doi:10.1097/ICU.0b013e3282c5077c.

[12] Char DH, Miller T, Kroll S. Orbital metastases: diagnosis and course. Br J Ophthalmol 1997; 81: 386–390. doi:10.1136/bjo.81.5.386. PMid:9227204.

[13] Shome D, Honavar SG, Raizada K, Raizada D. Implant prosthesis movement after enucleation: a randomized controlled trial. Ophthalmology 2010; 117: 1638–1644. doi:10.1016/j.ophtha.2009.12.035. PMid:20417565.

[14] Chou T, Siegel M. A mechanical model of retinal detachment. Phys Biol 2012; 9: 046001. doi:10.1088/1478-3975/9/4/046001. PMid:22733081.

[15] Haug SJ, Bhisitkul RB. Risk factors for retinal detachment following cataract surgery. Curr Opin Ophthalmol 2012; 23: 7–11. doi:10.1097/ICU.0b013e32834cd653. PMid:22081033.